Lawrence Berkeley National Laboratory
LBL Publications

Title

Energetics and the Role of Defects in Fe(II)-Catalyzed Goethite Recrystallization from Molecular Simulations

Permalink

https://escholarship.org/uc/item/9zj6x24m

Journal

ACS Earth and Space Chemistry, 3(2)

ISSN

2472-3452

Authors

Zarzycki, Piotr
Rosso, Kevin M

Publication Date

2019-02-21

DOI

10.1021/acsearthspacechem.8b00175

Peer reviewed

eScholarship.org Powered by the California Digital Library
University of California

Energetics and the Role of Defects in Fe(II)-Catalyzed Goethite Recrystallization from Molecular Simulations

Piotr Zarzycki[a*] and Kevin M. Rosso[b*]

[a]Energy Geosciences Division, Lawrence Berkeley National Laboratory, 1 Cyclotron Road, Berkeley, California 94720, United States

[b]Physical Sciences Division, Pacific Northwest National Laboratory, Richland, Washington, 99352, United States

KEYWORDS goethite, isotopic exchange, electron transfer, reductive dissolution, oxidative precipitation, Constant pH molecular dynamics, reactive Monte Carlo, surface defects, surface roughness

ABSTRACT: Goethite is one of the most stable and common iron (III) minerals at the Earth's near surface. However, recent isotope-tracer studies suggest that goethite continuously recrystallizes in the presence of aqueous Fe(II) ions. Such studies often indicate the presence of two regimes of atom exchange kinetics, a rapid stage assigned to reactive defect sites initially available at particle surfaces, followed by slower continuous exchange. An autocatalytic solid-state electron conduction model coupling Fe(II) oxidative adsorption to its reductive release at spatially distinct sites has been proposed, but the thermodynamic driving force has yet to be pinpointed. Here, using a novel hybrid/reactive molecular simulation method, for goethite (110) surfaces at circumneutral pH, we rigorously tested whether surface free energy minimization, including examining the role of structural defects, is sufficient to overcome the activation energy for interfacial electron transfer and conduction. The simulations quantitatively show that: i). on smooth stable surfaces the available thermal energy at dynamic equilibrium is sufficient to sustain the slow continuous regime of atom exchange kinetics via short intra-surface electron conduction pathways of 1-2 nm (3-5 Fe site hops); ii). in this slower regime, the model converges to atom exchange kinetics of 10^{-5} Fe s^{-1} cm^{-2}, a rate recently deduced from stochastic modeling of experimental data and linked to the reductive dissolution rate of goethite; iii). the driving force for initially rough defective goethite surfaces to smoothen can accelerate atom exchange to an extent quantitatively consistent with that observed in the initial rapid stage, in this case accessing conduction pathways of up to 8 nm. The findings suggest that the interaction of Fe(II) with initially defective goethite surfaces can drive, by the conduction model, atom exchange that is capable of recrystallizing the interiors of nanoscale particles, and that, closer to equilibrium on smooth surfaces, slower atom exchange continues in perpetuity but likely involving only the outermost atomic layers.

INTRODUCTION

Iron(III) oxide and oxyhydroxide minerals are one of the most ubiquitous components of soils and sediments, often dominating the reactive surface area as fine-grained coatings of secondary precipitates on primary grains. They comprise a key sorbent of heavy/trace metals and organic contaminants and nutrients.[1] Transformations of these phases from one mineral to another can occur in response to changes in environmental variables (e.g., temperature, pressure, pH, redox potential), impacting the retention and cycling of associated compounds.[1-4] Given their high thermodynamic stability, most of these transformations exhibit slow kinetics. However, rates are often much faster under reducing conditions where aqueous Fe(II) becomes stable. In this case soluble Fe(II) interacts with relatively insoluble Fe(III)-oxides that together can autocatalyze redox reactions at the interface. In particular, interfacial Fe(II)/Fe(III) electron exchange appears to be the basis for relatively rapid exchange of Fe and O atoms between the soluble and insoluble compartments, leading to facile recrystallization of these otherwise recalcitrant Fe(III) oxides and oxyhydroxides.[4-13]

The focus of the current study is on understanding the mechanism of this Fe(II)-catalyzed recrystallization in detail, using the Fe(III)-oxyhydroxide mineral goethite (α-FeOOH) as the key archetype. Goethite crystallites typically occur in nano-to-micron sized lath shaped "rods" bounded by {110} prismatic faces and {021} tips.[1] Because of their small size, microscopic processes occurring on individual particles are difficult to isolate. The majority of the experimental evidence to date is in the form of macroscopic batch isotope tracer studies,[5, 6, 8, 13] and bulk characterization of solids by Mössbauer spectroscopy[7, 14] and ex situ electron microscopy.[15] Iron isotope-tracer experiments suggest that aqueous Fe(II) triggers a complete recrystallization of goethite within a few days,[5-8, 13] even at circumneutral pH where its solubility product constant is no greater than approximately $10^{-5.9}$ μM.[1] Based on evidence for hematite that oxidative adsorption of Fe(II) can couple to reductive Fe(II) release by electrical conduction through the solid between crystallographically distinct faces,[16] a model comprised of these same steps was proposed to explain goethite recrystallization.[5] The main strength of the model is its ability to explain exchange of iron atoms between the solid and solution phases in a nominally 1:1 fashion by coupled oxidative growth and reductive dissolution on individual particles, without necessarily having to invoke changes in goethite

total mass or particle physical characteristics such as size or shape. The main weakness is that a thermodynamic driving force capable of overcoming the work of electron injection and conduction[12, 17] must be convincingly demonstrated, which has so far remained elusive.

In this regard, much emphasis has been placed on examining the evolution of goethite particle size and shape during recrystallization, because this behavior could yield critical clues.[5, 6, 18] Electron microscopy studies, which have been limited to ex situ measurements on particle ensembles, yield inconsistent conclusions ranging from no detectable change[5, 6] to a systematic decrease in particle aspect ratio.[18] The latter is consistent with preferred oxidative adsorption on {110} faces coupled to reductive dissolution of (021) faces connected by electron conduction along the Fe double-chains comprising the fast growth direction of goethite rods.[12] However, it remains unclear whether longer but higher mobility electron hopping pathways between nominally unlike faces (i.e., {110} to {021} faces) can outcompete shorter but lower mobility pathways between nominally identical {110} faces. It is also unclear whether or not surface free energy minimization, such as that associated with the progressive decrease in aspect ratio,[18] and/or increase in average particle size through Ostwald ripening is a thermodynamic driving force large enough to overcome the resistivity of electron transport through goethite.[11, 19, 20]

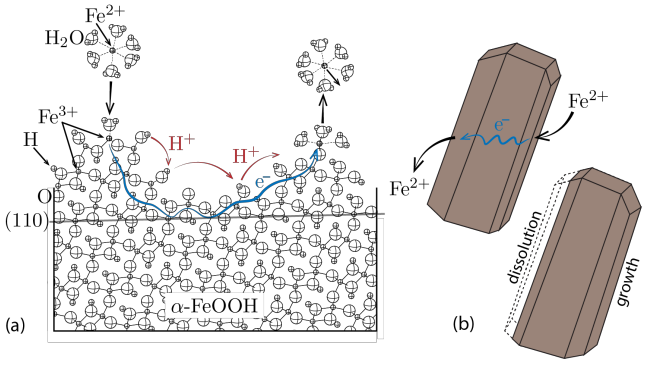

Figure 1. Illustration of the hypothesized iron atom exchange mechanism between aqueous Fe(II) and goethite surfaces (a): oxidative Fe(II) adsorption, electron transfer through the solid, and reductive dissolution of a distant solid Fe ion. In panel (b) we illustrate conceptually how this conduction mechanism of preferential dissolution and growth of the opposite faces of a particle is proposed to explain the mechanism of a complete-recrystallization without alteration of the aqueous/solid iron ratio.[5, 6]

The likely critical role of defects has recently come to light; the rate and extent of Fe atom exchange is now known to depend, at least initially, on the density of defects such as vacancies at the surface.[14, 17] With respect to the conduction model, it has been hypothesized that cation vacancies can serve as reactive sites for enhanced Fe(II) adsorption and electron injection into the solid, thereby facilitating atom exchange.[14] Recent Mössbauer experiments suggest that interfacial ET is more facile for cation-deficient goethite surfaces that are typical of goethite grown in low temperature aqueous solution.[14] However, it is also plausible that surface defects facilitate atom exchange simply by increasing the dissolution rate of the goethite surface. Stochastic simulations of measured tracer exchange data as a function of particle size and pH normalized to the sorbed Fe(II) density revealed an underlying atom exchange rate consistent with the expected reductive dissolution rate of goethite[11, 20] and not theoretically predicted interfacial electron transfer or conduction rates.[12] In the conduction model, this suggests that the rate limiting step in atom exchange is the last step in the electron transfer series – reduction of remote Fe(III) to Fe(II) and/or its detachment from the surface, processes that conceptually could be controlled by the availability of lower coordinated Fe sites at defective regions of the surface.

Here we report molecular simulations of the coupled evolution of the structure of goethite (110) crystal faces and Fe(II)-catalyzed atom exchange by the conduction mechanism. The goal is to specifically evaluate whether or not Gibbs free energy minimization of atomically rough, imperfect surfaces towards smooth ideal surfaces can drive electron conduction currents, and over what distances, that would enable the observed 1:1 atom exchange behavior. The modeling approach simultaneously accounts for and evolves the surface roughness and its associated electrostatic charge gradient at circumneutral pH with coupled growth and dissolution steps at two sites with probabilities proportional to the work required to link the two sites by interfacial electron transfer and conduction. Quantitative estimates of the thermodynamics and kinetics for individual steps were enabled by developing and applying a new hybrid reactive molecular simulation approach, which combines stochastic and deterministic simulation methods.

Specifically, our approach is based on enabling dynamic information passing between the cpHMD simulations of reactive surface structure and charge in water of Zarzycki et al.[19, 20] and kinetic Monte Carlo simulations of surface roughness evolution during 1:1 oxidative growth and reductive dissolution (referred as the KMC-cpHMD). This hybrid approach allowed us to explore the coupled dynamics of interacting surface electrostatics, formation and breakage of Fe-O bonds, and ET processes in a fully-atomistic setting and on a timescale approaching real experiments. The simulation is thus able to evaluate the balance of various competitive effects that yield the net driving force for atom exchange, such as surface free energy minimization versus conduction, and how various physicochemical gradients across goethite particles decay in time as the system evolves towards dynamic equilibrium.

This study is the first rigorous test of whether or not surface free energy minimization can drive the conduction model of Fe(II)-catalyzed atom exchange, as well as helping to constrain the possible role of surface defects. The results show that the driving force for surface free energy reduction readily overcomes the activation energy for electron injection and conduction over nanometer distances, leading to initially rapid 1:1 atom exchange within the first 24 h which later slows to an atom exchange rate controlled by the conduction mechanism alone, that continues to proceed even when the surface free energy is at dynamic equilibrium. The collective atom exchange kinetics and extents in the simulations are consistent with those reported in the batch tracer studies. Our simulation model is designed to be kinetically consistent with the previously reported the stochastic exchange model and its fit to experimental atom exchange data.[11] For instance, we find that the exchange rate in our KMC-cpHMD simulations converge to the nominal Fe-exchange rate of 10^{-5} Fe/nm^2/s as the surfaces reach dynamic equilibrium. [11]

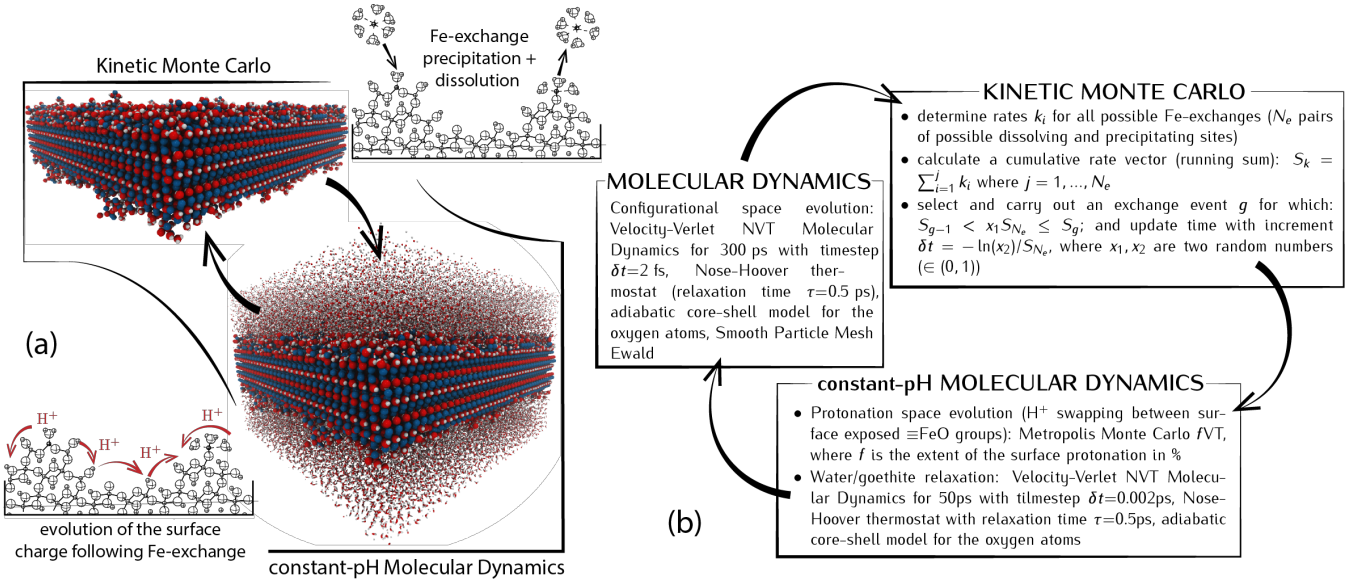

Figure 2. Hybrid simulation approach: (a) overview and (b) the key-algorithmic steps. Kinetic Monte Carlo simulation of Fe(II) exchange and surface morphological evolution, constant-pH molecular dynamics of the surface charge response to Fe(II) exchanges, and classical molecular dynamics simulation of the interfacial water response.

METHODS

Here we combine stochastic and deterministic simulation methods to sample simultaneously surface chemical transformations (dissolution, precipitation, evolution of the surface charge) and the time-evolution of atoms in configurational space. 1:1 dissolution and precipitation consistent with the conduction model are simulated using kinetic Monte Carlo (KMC), the proton uptake and release from the surface exposed hydroxy groups are simulated using constant-pH molecular dynamics (cpHMD) method, wherein the interfacial water and hydrogen-bond network reorganization are simulated by classical molecular dynamics (Fig. 2). For simplicity, water is treated explicitly only in the cpHMD and MD parts of the algorithm, by using the polarizable adiabatic-shell water model.[12] The force-field parameter values for the (110) goethite/water interface and Fe(II)/Fe(III) ions are taken from our previous studies.[12, 19, 20] The system was prepared by generating a goethite slab terminated by opposing (110) faces, the initial topography of which could be varied from perfectly flat terraces to atomistically rough by a random detachment of a subset of Fe atoms in the top layers and part of their coordination shells (Fig. 3); this procedure when applied progressively introduces the surface roughness on a length scale that in the extreme case is comparable with the slab thickness. The probability of Fe detachment we used was inversely proportional to the Fe-coordination, but purely random Fe removal and atom displacement were also implemented. The removed Fe atoms were not redeposited, leaving the surface corrugated and highly defective.

Kinetic Monte Carlo

KMC is an efficient sampling method that allows us to model the rare/slow events in the system, and to introduce a time-dependence to stochastic simulation.[21, 22] A key step in our KMC algorithm is calculation of the rate for each possible Fe-exchange event, which is based on the contributions of various coupled processes.

If Fe-detachment (dissolution) is taken as the rate-limiting step, the exchange rate is assumed to be proportional to the number of bonds that need to be broken (coordination of dissolving mineral building block j):[23]

$$k_{ij}^{exc} \equiv k_j^{dis} = A\exp\left(-\frac{z_j\varepsilon}{k_BT}\right) \quad (1)$$

where j is index of the dissolving fragment, z_j is coordination number and ε is the activation free energy for the dissolution (here breaking the Fe-O bond). Larger coordination numbers of the dissolving site equate to larger activation barriers and smaller dissolution (exchange) rates. Under these assumptions, Fe-exchange tends to progressively smoothen the surface due to the preferential execution of the fastest processes in the KMC-event pool (events with the lowest activation barriers and thus highest probabilities).

However, within the 1:1 exchange constraint, (reductive) dissolution is intimately coupled to (oxidative) precipitation. In this case, the total energy barrier thus depends on the number of bonds broken during the Fe-detachment step offset by the number of bonds formed (energy gain) in the Fe-attachment step. Specifically, we assume that the effective activation barrier is proportional to the coordination of the dissolving site (j) reduced by the coordination of the newly formed precipitate (i):

$$k_{ij} = A\exp\left(-\frac{(z_j - z_i)\varepsilon}{k_BT}\right) \quad (2)$$

where A is the effective frequency factor for dissolution, ε is the effective activation barrier for the Fe-exchange and Δz is a difference between the coordination of the goethite building blocks at the detachment (j) and attachment (i) sites (i.e., $\Delta z = z_j - z_i$). Rough surfaces can thus minimize their surface free energy by progressively reducing their broken bond densities by 1:1 dissolution-reprecipitation events. The rationale is that on rough surfaces the cost of breaking bonds for a reductive dissolution step is lowest at singly coordinated adatom sites, which is more than compensated by energy gained from formation of many new bonds by vacancy filling during oxidative Fe-attachment.

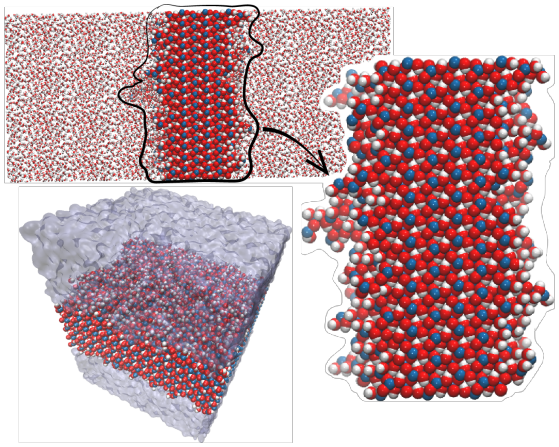

Figure 3. Illustration of simulation system: goethite slab terminated by randomly selected atomistically rough (110) surfaces (R_{RMS} =2.3 Å).

The difference in the local electrostatic environments of sites i and j is another factor influencing the exchange process. First, the protonated surface oxygen (≡FeOH, ≡$FeOH_2$) forms weaker bonds than deprotonated ones (≡FeO), a molecular basis for proton-promoted dissolution.[1] Second, deprotonated surface hydroxyls are more strongly electrostatically attractive to aqueous Fe(II), then protonated ones. Therefore, the activation barrier for the dissolution (precipitation) decreases (increases) with increasing protonation. Third, the local surface morphology dictates the electrostatic field in the vicinity of a given site. The atoms at surface kinks and step edges are more exposed to the solution and form weaker FeO bonds then those on the flat surface. [24] We take these effects into account by including the difference in the electrostatic energy between sites i and j ($e\Delta\psi_{j,i}$) in the rate definition:

$$k_{ij} = A\exp\left(-\frac{1}{k_BT}\underbrace{\left[(z_j - z_i)\varepsilon + e\Delta\psi_{j,i}\right]}_{\Delta G^{act}_{dis/prec}}\right) \quad (3)$$

where $\Delta\psi_{j,i}$ is the difference in the electrostatic (attraction) experienced by a probe charge at at position i and j. The electrostatic interactions are calculated within a 10 Å radius of a given site. The electrostatic contribution is negative for both sites, because the positive charge in the lattice position of Fe is stabilized by the surrounding anions (i.e., oxygen atoms) proportional to their protonation state. The electrostatic contribution introduces the correlation between the local surface protonation state (surface charge, σ_0) and the attachment and detachment processes beyond the first coordination shell of sites i and j.

Finally, the coupling between the oxidative precipitation and reductive dissolution process requires electron transfer from i-site (Fe(II)-oxidation to Fe(III) to j-site (surface Fe(III) reduction to Fe(II)). The energy cost of this charge transfer depends on the electron path and distance in the solid. We have shown previously that there are energetically favorable and unfavorable directions for electron transfer in the goethite structure.[12] In this work, we simplify the approach by only considering the length of the shortest electron-path from site i to j, that is a number of electron hops (n_{ET}). As we showed before, electron transfer in goethite occurs via thermally activated polaronic hops following the adiabatic formalism, due to the close proximity and strong electronic coupling between adjacent electron donor (Fe^{3+}) and acceptor (Fe^{2+}).[12, 20] In this model, the ET rate constant is given by:

$$k_{ET} = \nu\exp\left(-\frac{1}{k_BT}\left[\frac{(\Delta G_{ET}+\lambda)^2}{4\lambda} - V_{AB}\right]\right) \quad (4)$$

where ν is a frequency of vibrational mode acting along the nuclear reaction coordinate, λ is the reorganization energy, ΔG_{ET} is the ET free energy, and V_{AB} is an electronic coupling matrix element between reactants and products wave functions. To simplify the calculations, we use the average values of ET parameters for (110) goethite subsurface ET taken from our previous study:[12] ΔG_{ET}=0.335 eV, λ =2.17 eV, V_{AB} =0.1 eV and ν =1.39×10 ^{13} Hz; the corresponding average activation energy barrier for ET is thus taken as 24.238 k_BT. The time required for an electron to travel from site i to j is linearly proportional to the number of electron hops (n_{ET}), which translates to the following expression for the electron transfer rate constant:

$$k_{ij(ET)} = \frac{1}{n_{ET}}k_{ET} = \nu\exp\left(-\frac{1}{k_BT}\underbrace{\left[\frac{(\Delta G_{ET}+\lambda)^2}{4\lambda} - V_{AB} + k_BT\ln n_{FE}\right]}_{\Delta G^{act}_{ET}}\right) \quad (5)$$

Our final definition of the exchange kinetics contains various atomistic-level characterizations: the balance between broken and formed bonds, the balance between local charge states, electron transfer pathway and a possible external driving force consistent across the slab model (active if i and j are on the opposite side of the slab):

$$k_{ij}(z_i, z_j, \psi, n_{ET}, \dots) = A\exp\left(-\frac{1}{k_BT}\left[\Delta G^{act}_{dis/prec} + \Delta G^{act}_{ET} + \Delta G^{ext}\right]\right) \quad (6)$$

The dissolution-precipitation term favors recrystallization that smoothens the surface, the electron transfer term favors the shortest electron hopping pathway, and the external gradient can sustain directional particle recrystallization consistent with the conveyor-belt model. A solid-on-solid rule typical of MC simulations of surface growth or dissolution[23] was implemented to eliminate the prospect of the development of overhangs.

Kinetic Monte Carlo algorithm

There are several possible implementations of the KMC algorithm: residence-time Monte Carlo (also known as the rejection-free, n-fold way, or Bortz-Kalos-Lebowitz), rejection KMC and its cluster-variations (e.g., divide and conquer).[21, 22] Here we implemented residence-time KMC, in which a single Fe-exchange step is carried out in the following steps (Fig. 1b): (i) construct a set of all possible exchange events and their rates $\{k_1, k_2, \dots, k_N\}$ using eq. (6) for all surface exposed building blocks and all possible attachment sites (ii) generate a cumulative rate series $S_j = \sum_{i=1}^{j} k_i, j = 1, \dots, N$ and determine the i-event to carry out using a random number ($S_{u-1} < xS_N \le S_i$ where $x \in (0,1)$), (iii) carry out the i-exchange and update the time with an increment $\delta t = \ln(1/x')/S_N$ (where x' is another random number, $x' \in (0,1)$).

Our KMC procedure relies on recalculating the rate matrix every successful KMC step (each simulation run took about 800 hours using 16 CPU cores node Intel Xeon 2.6GHz node). More efficient KMC algorithms will be implemented in the future studies.

Parametrization of the exchange rate

Due to a lack of experimental data or accurate ab initio estimation of the Fe-O bond-forming/breaking activation energy we used arbitrary ε-values of 5, 8 and 10 k_BT, which are within a range of typical values for most minerals ($\varepsilon \in (4,11)$ k $_B$T see ref. [23]). Meakin and Rosso[23] pointed out that the activation barrier for the mineral dissolution can be even smaller due to the lattice strain-release around defects. The frequency factor (A) was obtained by scaling the averaged simulation exchange rate to the one extrapolated by fitting stochastic exchange model to the experimental exchange data:[11]

$$\langle \Delta t_{exp} \rangle = \langle \Delta t_{sim} \rangle / A \text{ where } \langle \Delta t_{sim} \rangle = \frac{1}{N_{KMC}} \sum_i^{N_{KMC}} \delta t \quad (7)$$

where δt is the KMC time increment, and N_{KMC} is the number of KMC steps.

Constant-pH Molecular Dynamics

In order to model the proton dynamics associated with Fe-exchange we implemented the constant-pH Molecular Dynamics algorithm, analogously to our previous report[19, 20] in which the protonation space is sampled using Monte Carlo and molecular dynamics is used to sample configurational space.[25, 26]

We prepare trial protonation microstates by swapping the protons between a few surface exposed oxygen atoms. At each attempt to change protonation state, we calculate the energy of this new trial surface protons configuration E_{new} and compare it to the energy of current proton distribution E_{old}. The new protonation state is accepted with the Metropolis-Hastings probability:

$$P(old \rightarrow new) = min\left\{1, exp\left(-\frac{E_{new}-E_{old}}{k_BT}\right)\right\} \quad (8)$$

The input geometry for each protonation state is optimized iteratively using the conjugate gradient algorithm until the change in energy is lower than 10^{-4} eV, then heated to 300K in NVT ensemble using the Berendsen thermostat (thermostat relaxation time 0.1 ps). The energies used in eq. (8) are the average configurational energies of system relaxed at T= 300K for the additional 10 ps. We used the velocity Verlet integrator with time step equals 0.2 fs. Next, the final protonation state obtained after 300-500 cpHMD steps (Fig. 4) was allowed to relax for another 50 ps using the classical molecular dynamics. Short-range interactions are neglected beyond 10 Å. Our program is written in the C++ language with parallelization provided by the Message Passing Interface (MPI) library.

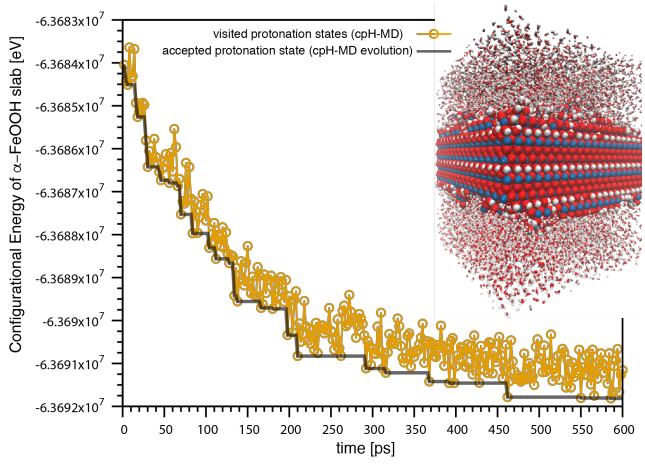

Figure 4. Typical surface charge evolution in the cpHMD algorithm: Monte Carlo sampling in the protonation space, among visited protonation states the one with the lowest configuration energy is used in the MD-part of cpHMD. Reorganization of the surface water for each protonation state is simulated using the classical molecular dynamics.

Polaron Pathway

We implemented Dijkstra's[27, 28] algorithm to find the shortest ET path between iron atoms i, j and to monitor the number of electron hops along that path (n_{ET}). The starting point i is the electron source (adsorbed, oxidized Fe(II)), and the end-point is the electron sink j (surface Fe(III)). In the graph theory terms,[28] Dijkstra's algorithm delivers the lowest-weight path between two given vertices in a network that have nonnegative weights, where the weights are Fe-Fe distances, and the vertices are Fe atoms.

Surface Roughness

We measure the evolution of the surface roughness during Fe-exchange using the root mean square roughness (R_{RMS}):[29]

$$R_{RMS} = \sqrt{\frac{1}{N}\sum_{i=1}^{N} h_i^2} \quad (9)$$

where the surface height (h_i) is the height of the peak or the depth of the valley defined as the distance between surface Fe atom i (z-coordinate in our case, z_i^{Fe}) and the surface baseline (i.e., an average z-coordinate of all top-layer Fe atoms, $\langle z^{\mathrm{Fe}} \rangle$).

Averaging Stochastic Exchange Pathways

We monitor several time-dependent characteristics ($f(t)$) of the evolving surfaces: net-growth and dissolution of surfaces ($\Delta N_{Fe}(t)$), surface roughness ($R_{RMS}(t)$), length of the ET-path and number of electron jumps ($l_{ET}(t)$, $n_{ET}(t)$). Because the KMC and MC selection processes are stochastic in nature, each simulation run provides slightly different time-dependent characteristics. The initial surface construction procedure (solid-on-solid KMC) is another source of randomness, because various atoms redistribution can provide the identical R_{RMS}.

To provide the most robust simulation data, we ran a number of simulations N_s for each of N_r initial surfaces, which have identical R_{RMS} but slightly different atomic distributions. The results presented here are the averages over all simulations runs and surfaces (i.e., $f(t) = \frac{1}{N_r N_s}\sum_i^{N_r} \sum_j^{N_s} f_{ij}(t)$ with $N_r = 12, N_s = 16$).

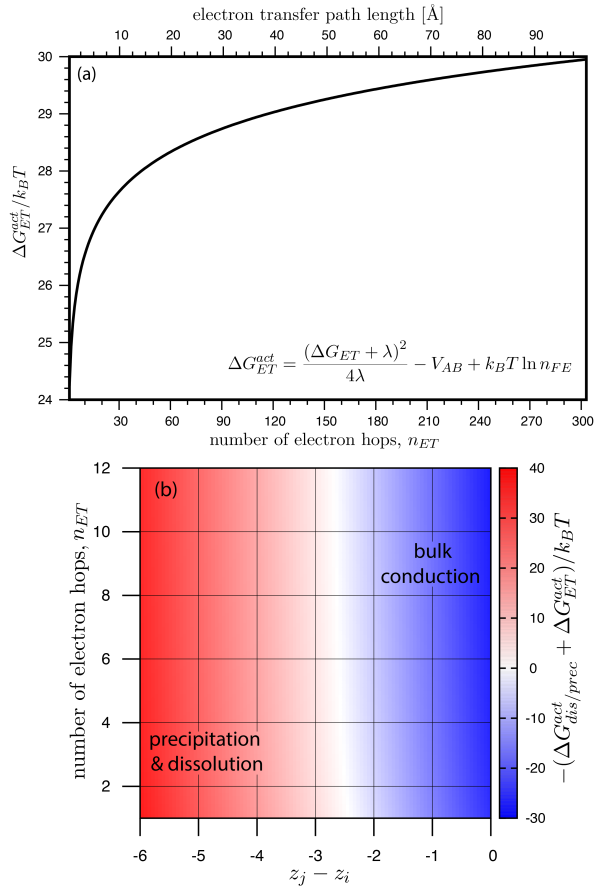

Figure 5. Bulk conduction contribution to the effective energy barrier for Fe-exchange as a function of electron transfer pathway length (a). For the conduction model[5] to operate, ΔG_{ET} corresponding to the particle width/length has to be compensated by the $\Delta G_{dis/pre}$ or ΔG^{ext}. In panel (b) we show two kinetic regimes visualized by plotting the exponential term in the thermally activated exchange rate expression ($-\Delta G^{acc}/k_Bt$) as function of the number of Fe-O bonds broken minus the number of the bonds formed ($z_j - z_i$) and the electron transfer pathway between sites i and j (i.e., number of ET hops, n_{ET}). The positive values (red) correspond to conduction-mediated atom exchange driven by surface free energy minimization (smoothening via dissolution/precipitation). The negative values (blue) correspond to the slow exchange governed by the electron hopping pathways in the oxide (bulk conduction). A single ET-step allows electron to travel on average 3-3.5 Å. The plot (b) was obtained for ε=10 k_BT, ψ=0, ΔG^{ext}=0.

RESULTS AND DISCUSSION

Model Assumptions and Initialization

One goal of the simulations was to evaluate the extent to which the activated kinetics of 1:1 atom exchange via the conduction mechanism could be driven by the minimization of surface free energy. To achieve this comprehensively the simulations were designed to be able to encompass situations when the initial surfaces were topographically rough (i.e., far from equilibrium) to topographically smooth (near equilibrium). In the former case a high density of undercoordinated Fe sites is present and a higher initial free energy associated with rough, defective surfaces is available. In the latter case, the driving forces available are those associated with rare event dissolution-reprecipitation processes thermally accessible at room temperature on smooth low-energy surfaces at dynamic equilibrium. In all cases, atomic rearrangements at the surface are only allowed to proceed by overcoming the activation energy of electron conduction through the goethite subsurface between two Fe sites - one undergoing oxidative Fe(II) adsorption and the other reductive Fe(II) release. Figure 3 depicts one representative goethite slab model bounded by two opposing (110) surfaces initialized with a selected amount of random roughness as described in the Methods section. Each surface possesses a distribution of Fe sites that have different coordination numbers to lattice O(H) atoms from 1 (adatom Fe) to 5 (terrace Fe), in each case having the remainder of Fe site hexacoordination fulfilled by H_2O/OH^- from solution.

Equation 6 introduces the effective energy barrier as a function of the difference in the number Fe-O (lattice) bonds broken and formed ($z_j - z_i$), the difference in local electrostatic energies at the two sites, the number of electron hops between the two sites (n_{ET}), and the external driving force. The first term preferentially favors dissolution of a site with the lowest number of bonds that need to be broken, e.g., an adatom site, and precipitation into sites of the opposite configuration, e.g., a vacancy site. The energy barrier decreases with increasing absolute magnitude of $z_j - z_i$. This introduces a proxy quantity for minimization of the surface free energy (i.e., minimization of the density of broken Fe-O bonds at the surface) that tends to drive initially rough surfaces to heal defects and evolve towards smooth dynamically stable surfaces. Another free energy driving force captured in our formulation is the difference in the local electrostatic environment of the two sites, which correlates with the differences in site coordination (z_i, z_j) and reflects the surface charge response to a change in the surface morphology. These two contributions are the only driving forces for Fe-exchange in the presented simulations. An option to include the influence of an additional external driving force, or barrier, is introduced only for the completeness of rate constant formalism, and in future work could be used to mimic effects such as a surface potential bias between crystallographically inequivalent terminations.[19, 20] Here we disregard such effects by setting $\Delta G^{ext} = 0$.

Energetic Competition Between Surface Smoothing and Bulk Conduction:

The collective driving forces for an Fe addition/removal step above are opposed by the work required to conduct electrons through goethite between the two selected sites. In constructing the matrix of KMC event rates every surface site i is connected with any other surface site j ($i \neq j$) in the Fe-addition/removal event with the exchange rate constant given k_{ij}. If the Fe-addition and removal sites are located on the opposite surfaces of the slab, the exchange process involves the conduction through the slab and it enables the roughness of both surfaces to diminish equally. On the other hand, if sites i,j are located on the same side of the slab it involves the conduction parallel to the surface and only one surface is smoothened during the Fe-exchange. The associated conduction (ET) work is always a positive contribution to the energy barrier due to the resistivity of site-to-site polaronic hopping, which increases with site separation distance. The magnitude of this contribution to the barrier is based on our prior molecular simulations of the direction-dependent site-to-site energy barriers to hopping in goethite (see Methods section). When treated as a sequence of hopping steps it turns out that this distance dependence goes as a logarithmic function of n_{ET} (Fig. 5a).

Because of the diminishing energy penalty for increasing multi-hop distances this allows longer-range conduction pathways to become a significant part of the sampling.

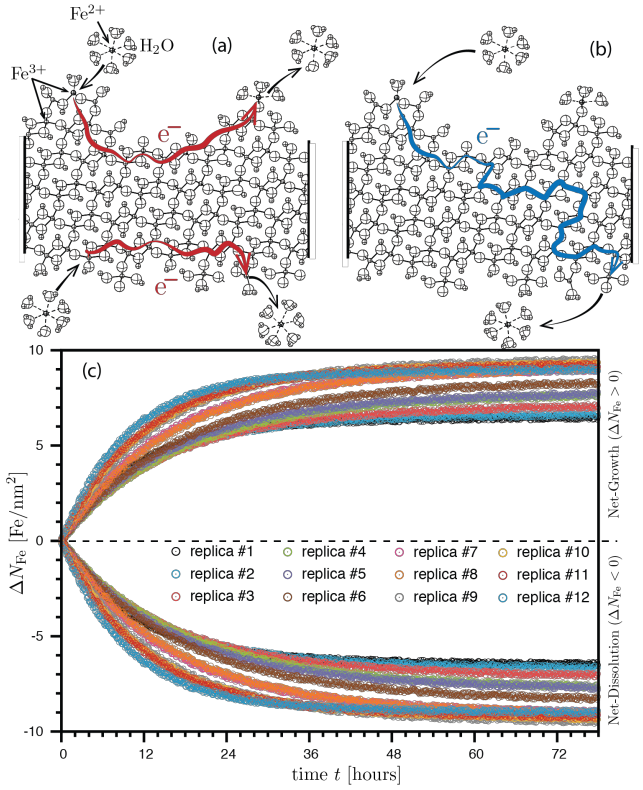

Figure 6. ET pathways: (a) electron source and sink are on the surface, Fe-loss due to the dissolution is balanced by Fe-gain due to the precipitation ($\Delta N_{Fe} = 0$), and (b) ET-across the goethite slab resulting in net-growth and net-dissolution ($\Delta N_{Fe} \neq 0$). In panel c, we showed averaged net-growth (initially 20% less rough surface) and dissolution (initially 20% more smooth surface) profiles for each surface replica. The FeO bond breaking/forming activation energies ε=5 k_BT. Each color represents an average of 16 simulation runs for any given initial surface configuration (i.e., replica).

Figure 5b summarizes the net balance between the opposing atom exchange forces of surface free energy minimization versus conduction. In brief, our simulations suggest that atom exchange by the conduction mechanism is thermally accessible on a time scale consistent with measured atom exchange kinetics irrespective of the surface free energy driving force contribution; the latter is, however, capable of accelerating the atom exchange rate. If the energy gain due to the surface smoothening and the energetic penalty due to the resistive conduction cancel each other, the exchange rate approaches the nominal Fe-exchange rate of 10^{-5} Fe/nm^2/s.[11] In Figure 5b we can distinguish two atom exchange domains in $z_j - z_i$ versus n_{FE} space: one in which the surface energy minimization contribution is large, i.e., the surfaces are rough, and the rate is not limited by the conduction process, and another domain in which the surface energy minimization driving force is low, i.e., the surfaces are smooth, and atom exchange continues at a rate defined by the work of conduction. The former represents a domain where 1:1 atom exchange mediated by conduction is accelerated by the driving force of surface energy minimization. In the latter domain atom exchange kinetics are defined by the rate of conduction. The boundary region represents a situation in which they cancel each other resulting in an activationless Fe-exchange process (effective activation barrier equals 0).

Comparing Intra- and Intersurface Atom Exchange:

In the rejection-free KMC algorithm the probability of selecting a given exchange event is proportional to its rate constant, however the slow exchange pathways (rare events) are also sampled. There is no inherent restriction on the type of the allowed exchange event. In order to gain an independent insight into the evolution of surfaces during Fe-exchange, we distinguished two cases of ET pathways in analyzing simulation data: one with the electron source and sink localized on the same side of the slab (Fig. 6a), and another with the source and sink on opposite sides of the slab during the exchange event (Fig. 6b). Over time both types of ET pathways enable simultaneous smoothing of both sides of the slab, however the latter case also enables mass transfer between surfaces via dissolution on one side and the precipitation on the other. If slab surfaces have the identical initial roughness there is a negligible net-mass transfer between surfaces because there is no driving force for the preferential dissolution and precipitation of the opposite surfaces of the slab. However, the slab can be initialized with different amounts of roughness on one side versus the opposing one. In such cases the mass transfer is proportional to the difference in the surface roughness.

If exchange events occur at one side of the slab they do not contribute to the net mass transfer from one side of the slab to the other ($\Delta N_{Fe} = 0$); this represents a case where exchange does not lead to net growth or dissolution of a goethite crystallite, but still smoothens the surface. If the exchange events couple one side of the slab to the opposite side, a higher amount of roughness on one side versus the other can lead to net mass transfer of Fe across the slab ($\Delta N_{Fe} \neq 0$), consistent with net growth and dissolution of coupled surfaces by conduction-based atom exchange. The latter case is discussed in terms of the surface-area-normalized difference between the number of precipitation and dissolution events for a given surface.

In Fig. 6c, we show averaged simulation results from 12 replications of the initial slab, each initialized with an identical roughness gradient from one side to the other (20%) and absolute roughness parameters R_{RMS}, but varying slightly in the actual atomic configuration. The simulation results were obtained for FeO-bond breaking/forming activation energy (ε) equal to 5 k_BT. Each replica simulation represents the average over 16 simulations starting from the same initial configuration, but with a different time-evolution due to the stochastic steps (KMC and MC part of the cpHMD).

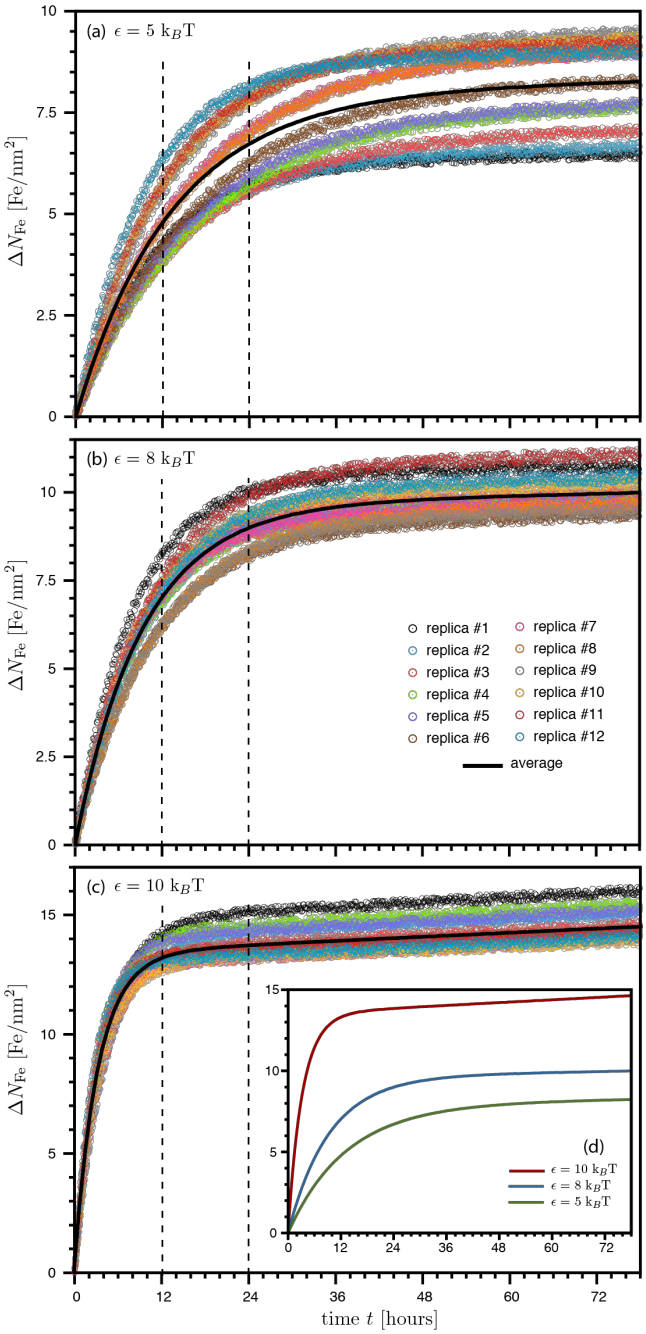

Figure 7. Net-growth of initially less rough surface (by 20%) for three different FeO bond breaking/forming activation energies (ε). The simulation results averaged for each replica are shown as circles. The average growth (black solid lines in a-c, and insert d) are the numerical averages over all simulation runs and replicas.

We observe the net-growth and net-dissolution of surfaces only if there is a roughness gradient between surfaces. The surface that was initially rougher preferentially dissolves ($\Delta N_{Fe} < 0$), whereas the one that was smoother grows ($\Delta N_{Fe} > 0$). The net-growth and net-dissolution are rapid (exponential) within first 24 hours, and then become very slow (Fig. 6c). If the surfaces have identical roughness, they still smoothen via Fe-exchange, but statistically without any mass transfer ($\Delta N_{Fe} = 0$, results not shown).

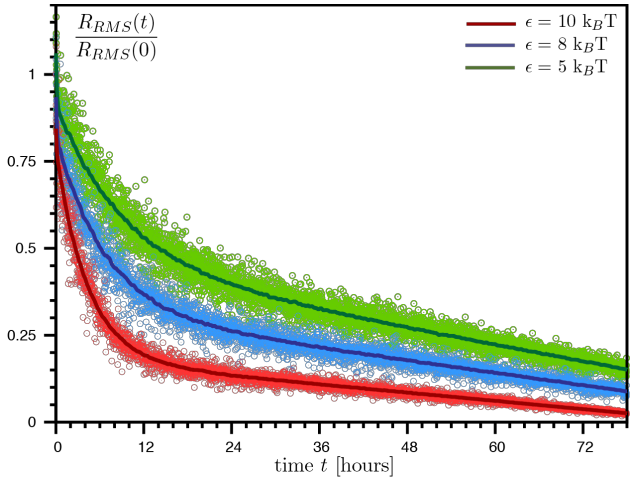

Figure 8. Evolution of the average root-mean-square surface roughness for three different FeO bond breaking/forming activation energies (ε). R_{RMS} is an average for two surfaces of the slab, and represents the smoothening driven by the Fe-exchange. The initial root-mean square surface roughness is equal to $R_{RMS}(0)$=7.2 Å.

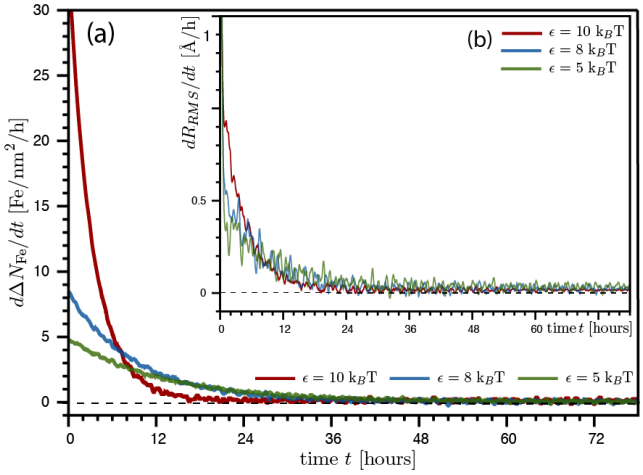

Figure 9. Rate of growth/dissolution (a) and smoothening (b) for for three different FeO bond breaking/forming activation energies (ε).

In Fig. 7 we compare the simulation results of the net-growth of the initially less rough surface for FeO-bond activation energies equal to 5, 8 and 10 k_BT. By comparing the variation within the averaged simulations for each replica, we find that with larger values of ε the dependence of ΔN_{FE} on $z_j - z_i$ becomes stronger and the susceptibility to thermal fluctuations becomes weaker. The extent and rate of net-growth (net-dissolution) are also proportional to ε (Fig. 7d), because for larger values of ε the energy gain due to FeO bond formation overcomes the cost of conduction across the slab. In all three cases (Fig. 7a-c) we observe the fast-initial growth/dissolution driven by Fe-exchange, which become slow at time depending on ε. The transition between fast and slow growth/dissolution regimes occur around 6 (ε= 10 k_BT), 18 (ε= 8 k_BT) and 26 hours (ε= 5 k_BT).

Our results suggest that the smaller FeO-bond activation energy the slower growth-dissolution is driven by the roughness gradient. This is a surprising result - a consequence of

assuming that the FeO-bond formation and breaking have similar activation barrier (ε).

In Fig. 8 we show the slab-averaged surface smoothening profiles ($R_{RMS}(t)/R_{RMS}(0)$) as a function of time and Fe-bond activation energies. Although the time-evolution of roughness shows a similar kinetic dichotomy, it is less sensitive to ε. In addition, the surfaces smoothen even when the net-growth/dissolution becomes negligible (Fig. 6 t >30 hours). The surfaces smoothening without net-growth and net-dissolution is an indication of the dominance of intra-surface charge transfer (Fig. 6a).

By comparing the rate of net-growth/net-dissolution (Fig. 9a) and the rate of surface smoothening (Fig. 9b) we prove that surface morphology evolves at constant (>0) rate even when the rate net-growth/net-dissolution is negligible (~0). In addition, the rate of surface smoothing is less sensitive to ε than net-growth/dissolution. This is because the morphological evolution of the surface does not require long charge transfer distances across the slab.

This suggests that the ET-path should shorten over time, as the energy gain due to the formation of FeO-bonds and electrostatic energy minimization are not sufficient to sustain the resistive conduction through slab. Indeed, by analyzing the length of the electron transfer pathways as a function of time we observe a transition from the wide spectrum of ET-pathways to a very narrow distribution of short pathways (Fig. 10). ET across goethite particles should therefore be more frequent if surfaces are rough/defective, and in particular, if there is a gradient in the surface topographic properties across the slab.

The sensitivity of the distributions to the value of ε are more pronounced within the first 24 hours (Fig. 10a), but present also for slower kinetics (Fig. 10b). The change in the ET-pathway distribution, net-growth/dissolution, and smoothing are a consequence of the change in the Fe-exchange energetics. Initially, the difference in surface roughness is a primary driving force for Fe-exchange, consistent with the finding that presence of surface defects increase the extent of Fe-exchange.[14] As soon as the surfaces become smooth, the rate of Fe-exchange is low and inversely proportional to the ET length.

Our simulations show that the process of 1:1 atom exchange mediated by conduction turns out to be energetically and kinetically accessible within the time scale of batch tracer exchange measurements across all conditions considered. The findings are consistent with previous studies, in which the initial rapid Fe-exchange turns into slower-kinetic regimes after first day.[9-11] However, by using molecular simulation methods we were able for the first time to provide an atomistic-level connection between the change in the atom exchange reactivity and the evolution of surface morphology and charge.

Even though we simulated a goethite slab that is thinner (2-3 nm) than goethite particle dimensions used in most prior experimental studies,[5, 6] we were able to show that in the absence of any external driving force, a gradient in surface properties such as roughness, or defect content, is sufficient to drive preferential dissolution and precipitation of mirrored faces of the particle. Previously, we also showed that spontaneously arising electrostatic voltage between surfaces can provide an additional driving force for the conduction model. Collectively, we find that the rapid initial Fe-exchange is due to the initial reactivity of imperfect goethite particle surfaces. The simulations presented here show that initially rapid Fe-catalyzed recrystallization results in the formation of more inert (e.g., smooth and less-defective) surfaces within 24 hours. However, because the current simulation protocol is too computationally expensive to encompass entire goethite nanorods bearing inequivalent crystallographic terminations, we are yet unable to address processes sustained over longer time scales that can lead to complete recrystallization and progressive particle shape evolution.

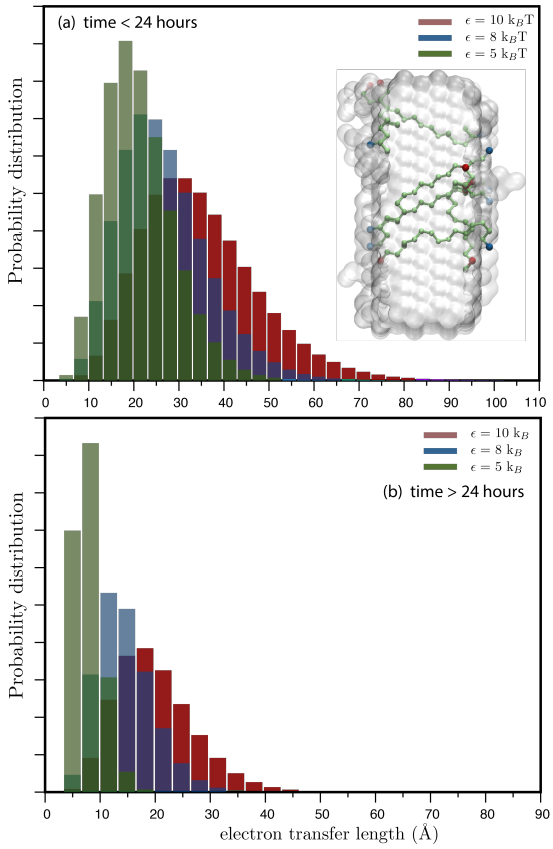

Figure 10. Distribution of the ET-pathway length for systems with surfaces-roughness disproportionality (20%) and various FeO-bond breaking/forming activation energy (ε): within 24 hours (a), and after first 24 hours (b). The ET-length is approximated by shortest path between sites i and j using the Dijkstra's algorithm[28] considering Fe atoms as the network nodes (a few paths visualized in the insert). The histogram bin equals 3.3Å - an average length of a single ET-step.

Conclusions

Using novel molecular simulation methods, we were able for the first time to provide an rigorous connection between macroscopically observed atom exchange behavior and goethite particle reactivity and morphology evolution at the atomic scale. Largely in support of the mechanistic speculation in prior studies,[9-11] our simulations show two kinetic domains: rapid initial exchange within 24 hours followed by a slow near-equilibrium exchange. Surface defects and initial roughness accelerate Fe-exchange, accessing long electron conduction pathways (≤80Å) and enabling coupled dissolution and precipitation of opposing goethite (110) crystal faces - consistent with the original assumptions of the conduction model[5] - but only for the first 24 hours of Fe-exchange. As surface free energies and average gradients across particle are minimized, to the extent that only short electron pathways remain

energetically accessible (≤20Å). Differences in the local surface protonation drive these short-range electron transfers, and in this sense these atom exchange processes at dynamic equilibrium limit atom exchange to the outermost surface atoms and do not have a preferred crystallographic direction that could sustain a morphology change. This is consistent with tracer studies that suggest only surface ^{57}Fe-enrichment over longer time scales, and particle recrystallization limited to the initially rough reactive surfaces.

On the other hand, there are energetically favorable electron pathways in goethite.[12] These pathways do not connect the dominant crystal faces of particles - but allow charge to migrate along the doubly-coordinated (O-bridged) Fe atoms parallel to the (110) surface.[12] If these favorable charge pathways are combined with the short-range resistive currents sustained by the differences in local protonation states, the surfaces of the goethite particle are electronically coupled (a long-range subsurface conduction model). This connection and the existence of the intrinsic energy gradient between surfaces are essential to fully rationalize the conduction model.[5]

AUTHOR INFORMATION

Corresponding Author

*e-mail: ppzarzycki@lbl.gov (PZ), kevin.rosso@pnnl.gov (KM)

Author Contributions

The manuscript was written through contributions of all authors. / All authors have given approval to the final version of the manuscript.

Funding Sources

This material is based upon work supported by the U.S. Department of Energy, Office of Science, Office of Basic Energy Sciences, Chemical Sciences, Geosciences, and Biosciences Division, through its Geosciences program at Pacific Northwest National Laboratory and at Lawrence Berkeley National Laboratory (under contract DEAC02-05CH11231).

ACKNOWLEDGMENT

We thank Benjamin Gilbert (LBNL) for insightful comments. This material is based upon work supported by the U.S. Department of Energy, Office of Science, Office of Basic Energy Sciences, Chemical Sciences, Geosciences, and Biosciences Division, through its Geosciences program at Pacific Northwest National Laboratory and at Lawrence Berkeley National Laboratory (under contract DE-AC02-05CH11231).

REFERENCES

1. Schwertman, U.; Cornell, R. M., *The Iron Oxide. Structure, Properties, Reactions, Occurrence and Uses*. Wiley: Weinheim, 2003.
2. Scherer, M. M.; Balko, B. A.; Tratnyek, P. G., The Role of Oxides in Reduction Reactions at the Metal-Water Interface. In *Mineral-Water Interfacial Reactions*, American Chemical Society: 1999; pp 301–322.
3. Cwiertny, D. M.; Hunter, G. J.; Pettibone, J. M.; Scherer, M. M.; Grassian, V. H., Surface Chemistry and Dissolution of alpha-FeOOH Nanorods and Microrods: Environmental Implications of Size-Dependent Interactions with Oxalate. *J Phys Chem C* **2009,** *113* (6), 2175-2186.
4. Latta, D. E.; Gorski, C. A.; Scherer, M. M., Influence of Fe^{2+}-catalysed iron oxide recrystallization on metal cycling. *Biochem Soc T* **2012,** *40*, 1191-1197.
5. Handler, R. M.; Beard, B. L.; Johnson, C. M.; Scherer, M. M., Atom Exchange between Aqueous Fe(II) and Goethite: An Fe Isotope Tracer Study. *Environ Sci Technol* **2009,** *43* (4), 1102-1107.
6. Handler, R. M.; Frierdich, A. J.; Johnson, C. M.; Rosso, K. M.; Beard, B. L.; Wang, C. M.; Latta, D. E.; Neumann, A.; Pasakarnis, T.; Premaratne, W. A. P. J.; Scherer, M. M., Fe(II)-Catalyzed Recrystallization of Goethite Revisited. *Environ Sci Technol* **2014,** *48* (19), 11302-11311.
7. Williams, A. G. B.; Scherer, M. M., Spectroscopic evidence for Fe(II)-Fe(III) electron transfer at the iron oxide-water interface. *Environ Sci Technol* **2004,** *38* (18), 4782-4790.
8. Beard, B. L.; Handler, R. M.; Scherer, M. M.; Wu, L. L.; Czaja, A. D.; Heimann, A.; Johnson, C. M., Iron isotope fractionation between aqueous ferrous iron and goethite. *Earth Planet Sc Lett* **2010,** *295* (1-2), 241-250.
9. Gorski, C. A.; Fantle, M. S., Stable mineral recrystallization in low temperature aqueous systems: A critical review. *Geochim Cosmochim Ac* **2017,** *198*, 439-465.
10. Joshi, P.; Fantle, M. S.; Larese-Casanova, P.; Gorski, C. A., Susceptibility of Goethite to Fe^{2+}-Catalyzed Recrystallization over Time. *Environ Sci Technol* **2017,** *51* (20), 11681-11691.
11. Zarzycki, P.; Rosso, K. M., Stochastic Simulation of Isotopic Exchange Mechanisms for Fe(II)Catalyzed Recrystallization of Goethite. *Environ Sci Technol* **2017,** *51* (13), 7552-7559.
12. Zarzycki, P.; Kerisit, S.; Rosso, K. M., Molecular Dynamics Study of Fe(II) Adsorption, Electron Exchange, and Mobility at Goethite (alpha-FeOOH) Surfaces. *J Phys Chem C* **2015,** *119* (6), 3111-3123.
13. Gorski, C. A.; Scherer, M. M., Fe^{2+} Sorption at the Fe Oxide-Water Interface: A Revised Conceptual Framework. In *Aquatic Redox Chemistry*, American Chemical Society: 2011; Vol. 1071, pp 315–343.
14. Notini, L.; Latta, D. E.; Neumann, A.; Pearce, C. I.; Sassi, M.; N'Diaye, A. T.; Rosso, K. M.; Scherer, M. M., The Role of Defects in Fe(II)-Goethite Electron Transfer. *Environ Sci Technol* **2018,** *52* (5), 2751-2759.
15. Taylor, S. D.; Liu, J.; Arey, B. W.; Schreiber, D. K.; Perea, D. E.; Rosso, K. M., Resolving Iron(II) Sorption and Oxidative Growth on Hematite (001) Using Atom Probe Tomography. *J Phys Chem C* **2018,** *122* (7), 3903-3914.
16. Yanina, S. V.; Rosso, K. M., Linked reactivity at mineral-water interfaces through bulk crystal conduction. *Science* **2008,** *320* (5873), 218-222.
17. Alexandrov, V.; Rosso, K. M., Electron transport in pure and substituted iron oxyhydroxides by small-polaron migration. *J Chem Phys* **2014,** *140* (23).
18. Joshi, P.; Gorski, C. A., Anisotropic Morphological Changes in Goethite during Fe2+-Catalyzed Recrystallization. *Environ Sci Technol* **2016,** *50* (14), 7315-7324.
19. Zarzycki, P.; Smith, D. M.; Rosso, K. M., Proton Dynamics on Goethite Nanoparticles and Coupling to Electron Transport. *J Chem Theory Comput* **2015,** *11* (4), 1715-1724.
20. Zarzycki, P.; Rosso, K. M., Surface Charge Effects on Fe(II) Sorption and Oxidation at (110) Goethite Surfaces. *J Phys Chem C* **2018,** *122* (18), 10059-10066.
21. Newman, M. E. J.; Barkema, G. T., *Monte Carlo Methods in Statistical Physics*. Oxford University Press: Oxford 1999.
22. Jansen, A. P. J., *An Introduction to Kinetic Monte Carlo Simulations of Surface Reactions*. Springer: Berlin, 2012.
23. Meakin, P.; Rosso, K. M., Simple kinetic Monte Carlo models for dissolution pitting induced by crystal defects. *J Chem Phys* **2008,** *129* (20).
24. Rustad, J. R.; Felmy, A. R., The influence of edge sites on the development of surface charge on goethite nanoparticles: A molecular dynamics investigation. *Geochim Cosmochim Ac* **2005,** *69* (6), 1405-1411.
25. Mongan, J.; Case, D. A.; McCammon, J. A., Constant pH molecular dynamics in generalized born implicit solvent. *J Comput Chem* **2004,** *25* (16), 2038-2048.

26. Mongan, J.; Case, D. A., Biomolecular simulations at constant pH. *Curr Opin Struc Biol* **2005,** *15* (2), 157-163.
27. Mehlhorn, K. S., P., *Algorithms and Data Structures: The Basic Toolbox*. Springer: Berlin, 2008.
28. Sedgewick, R., *Algorithms in C++ Part 5: Graph Algorithms*. Addison-Wesley: Boston, 2002.
29. LaMarche, C. Q.; Leadley, S.; Liu, P. Y.; Kellogg, K. M.; Hrenya, C. M., Method of quantifying surface roughness for accurate adhesive force predictions. *Chem Eng Sci* **2017,** *158*, 140-153.

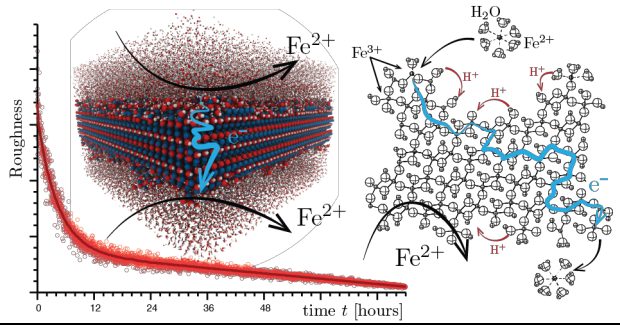
Roughness
time t [hours]
0
12
24
36
48
Fe^{2+}
e^-
Fe^{2+}
H_2O
Fe^{3+}
Fe^{2+}
H^+
H^+
H^+
H^+
e^-
Fe^{2+}